Photodiagnosis and Photodynamic Therapy 40 (2022) 103199

Contents lists available at ScienceDirect

Photodiagnosis and Photodynamic Therapy

journal homepage: www.elsevier.com/locate/pdpdt

Surface-enhanced Raman spectroscopy for characterization of filtrate portions of blood serum samples of typhoid patients

Maria Akram [a], Muhammad Irfan Majeed [a,*], Haq Nawaz [a,*], Nosheen Rashid [b,*], Muhammad Rizwan Javed [c], Muhammad Zeeshan Ali [a], Ali Raza [a], Muhammad Shakeel [a], Hafiz Mahmood ul Hasan [a], Zain Ali [a], Usama Ehsan [a], Muhammad Shahid [a]

[a] Department of Chemistry, University of Agriculture Faisalabad, Faisalabad 38000, Pakistan
[b] Department of Chemistry, University of Education, Faisalabad Campus, Faisalabad 38000, Pakistan
[c] Department of Bioinformatics and Biotechnology, Government College University Faisalabad (GCUF), Faisalabad 38000, Pakistan

ARTICLE INFO

Keywords:
Surface-enhanced Raman spectroscopy
Typhoid
Blood serum
Centrifugal filtration
Silver nanoparticles
Chemometrics

ABSTRACT

Background: Surface-enhanced Raman spectroscopy (SERS) is explored to design a rapid screening method for the characterization and diagnosis of typhoid fever by employing filtrate fractions of blood serum samples obtained by centrifugal filtration with 50 KDa filters.

Objectives: The purpose of this study, to separate the filtrate portions of blood serum samples in this way contain proteins smaller than 50 kDa and removal of bigger size protein which allows to acquire the SERS spectral features of smaller proteins more effectively which are probably associated with typhoid disease. Disease caused by *Salmonella typhi* diagnose more effectively by using surface-enhanced Raman spectroscopy (SERS) and multivariate data analysis tools.

Methods: SERS was used as a diagnostic tool for typhoid fever by comparison between healthy and diseased samples. For this purpose, all the samples were analyzed by comparing their SERS spectral features. Over the spectral range of 400-1800cm^{-1}, multivariate data analysis techniques such as Principal Component Analysis (PCA) and Partial Least Squares-Discriminant Analysis (PLS-DA) are applied to diagnose and differentiate different filtrate fractions of blood serum samples of patients of typhoid fever and healthy ones.

Results: By comparing SERS spectra of healthy filtrate with that of filtrate of typhoid sample, the SERS spectral features associated with disease development are identified including PCA is found to be efficient for the qualitative differentiation of all of the samples analyzed. Moreover, PLS-DA successfully identified and classified healthy and typhoid positive blood serum samples with 97 % accuracy, 99 % specificity, 91 % sensitivity and 0.78 area under the receiver operating characteristic (AUROC) curve.

Conclusions: Surface enhanced Raman spectroscopy using silver nanoparticles SERS substrate, is found to be useful technique for the quick identification and evaluation of filtrate fractions of the blood serum samples of healthy and typhoid samples for disease diagnosis.

1. Introduction

Typhoid infection is an infectious [1] and mortal disease [2] caused by a host-adapted, gram-negative, human-specific pathogen that belongs to the *Enterobacteriaceae* family of aerobic, rod-shaped, flagellated bacterium *Salmonella enterica serovar typhi* [3]. Typhoid fever is a leading source of mortality in developing countries. Annually, an estimated 26.9 million cases and around 217,000 mortalities are observed [4]. The *Salmonella* bacteria can survive at temperatures ranging from 5 to 45 °C, with a preferred temperature of 35–37°C. It grows best in a pH range of 6 to 7, however, it may also grow at pH 4.1 [5]. The fecal-oral route is the most common way of infection. It is a foodborne disease that is spread by the ingestion of infected animal products such as meat, dairy, poultry, fish (tuna), as well as eggs [6].

Salmonella typhi is present in the bloodstream of the infected people and intestinal tract and periodically "discharges" the bacteria in their feces, less usually in their urine [7]. Typhoid fever has a higher risk of mortality of up to 10%. The bacterium is excreted from the gallbladder

* Corresponding authors at: Department of Chemistry, University of Agriculture Faisalabad, Faisalabad, Other 38000, Pakistan.
E-mail addresses: irfan.majeed@uaf.edu.pk (M.I. Majeed), haqchemist@yahoo.com (H. Nawaz), nosheenrasheed@yahoo.com (N. Rashid).

https://doi.org/10.1016/j.pdpdt.2022.103199
Received 24 August 2022; Received in revised form 2 November 2022; Accepted 8 November 2022
Available online 9 November 2022

for months to years in chronic carriers [8]. Although various microbial serological techniques like blood culture and Widal test [9], Typhidot (IgM) for early diagnosis [10], enzyme-linked immunosorbent assay (ELISA) [11], Loop-mediated isothermal amplification [12], biosensors and polymerase chain reactions (PCR) [13] are applied to identify typhoid disease they are limited by low specificity and time consumption [14]. Furthermore, because of the similarities in persistent fever and other clinical signs, it is challenging to distinguish typhoid fever from other illnesses for instance paratyphoid (A, B, C) as well as pneumonia, which requires sensitive, specific, reproducible, and reliable diagnostic procedures [15]. Raman spectroscopy (RS) has been found as a possible analytical technique for detecting water-borne pathogens. It is inexpensive, has high content information, and can analyze biochemical changes caused by microbes during the development of infection, quickly. RS is a form of vibrational molecular spectroscopy that may be used to analyze materials quantitatively and qualitatively [16]. Since biological molecules such as protein, DNA/RNA, and hemoglobin have low concentrations in body fluids hence give weak Raman spectroscopy signals which make their identification difficult. To identify such molecules in biological fluids at low concentrations, SERS is used to enhance the Raman signal of molecules using metallic nanoparticles as SERS substrates. Using nanoparticles as the SERS substrate is the typical method for enhancing the Raman signal. With a limit of detection (LOD) as low as a single cell, SERS coupled with silver nanoparticles (Ag NPs) has shown potential for rapidly and precisely identifying and differentiating bacteria [17–22]. Silver nanoparticles were utilized as a SERS substrate in this analysis to enhance the Raman signal. Silver (Ag) and gold (Au) NPs have the maximum SERS enhancement factor due to their strong surface plasmon characteristics. The silver-NPs have been widely used as an effective substrate. The SERS examination of various microbes is reported in multiple research reports [17,23-34]. The SERS enhancement is greater with Ag-nanoparticles than with Au-nanoparticles due to the enhanced surface plasmon response due to a higher number of available active sites (hotspots). They are also simple to make and inexpensive [17,35].

In this work, filtrate fractions of blood serum samples of typhoid-positive also healthy individuals are obtained by employing 50 KDa filters as depicted in Fig. 1. Human blood serum is a complex mixture of lipids, proteins amino acids, and carbohydrates [36]. High molecular weight fraction (HMWF) biomolecules are more abundant while low molecular weight fraction (LMWF) biomolecules are less abundant in the blood serum. Larger proteins with high molecular weights, such as albumin (50-60%) and globulin (40%) of the overall protein content of serum [37], dominate smaller proteins and other biomolecules including carbohydrates, lipids, amino and nucleic acids called LMWF. The identification of potentially significant disease biomarkers is made more challenging by the existence of the HMWF in serum. To solve this problem, HMWF and low molecular weight (LMWF) fractions are separated using centrifugal filter devices with varying molecular weight cut-offs [38]. It is possible to detect changes in the LMWF by separating these proteins like albumin and globulins [39–41]. Centrifugal filtration for the separation of the low and high-molecular-weight fractions from serum samples of typhoid fever is followed by Surface Enhanced Raman Spectroscopy.

Six proteins make up around 90% of the serum's total protein contents. Each one weighs more than 50 kDa. These proteins are Albumin (66 kDa), immunoglobulin G (IgG) with 150 kDa, transferrin (80 kDa), α1-Antitrypsin (52 kDa), immunoglobulin A (IgA) 180-500 kDa and immunoglobulin M (IgM) (950 kDa) [41,42].In this study, the authors used a 50 kDa filter because a majority of Salmonella

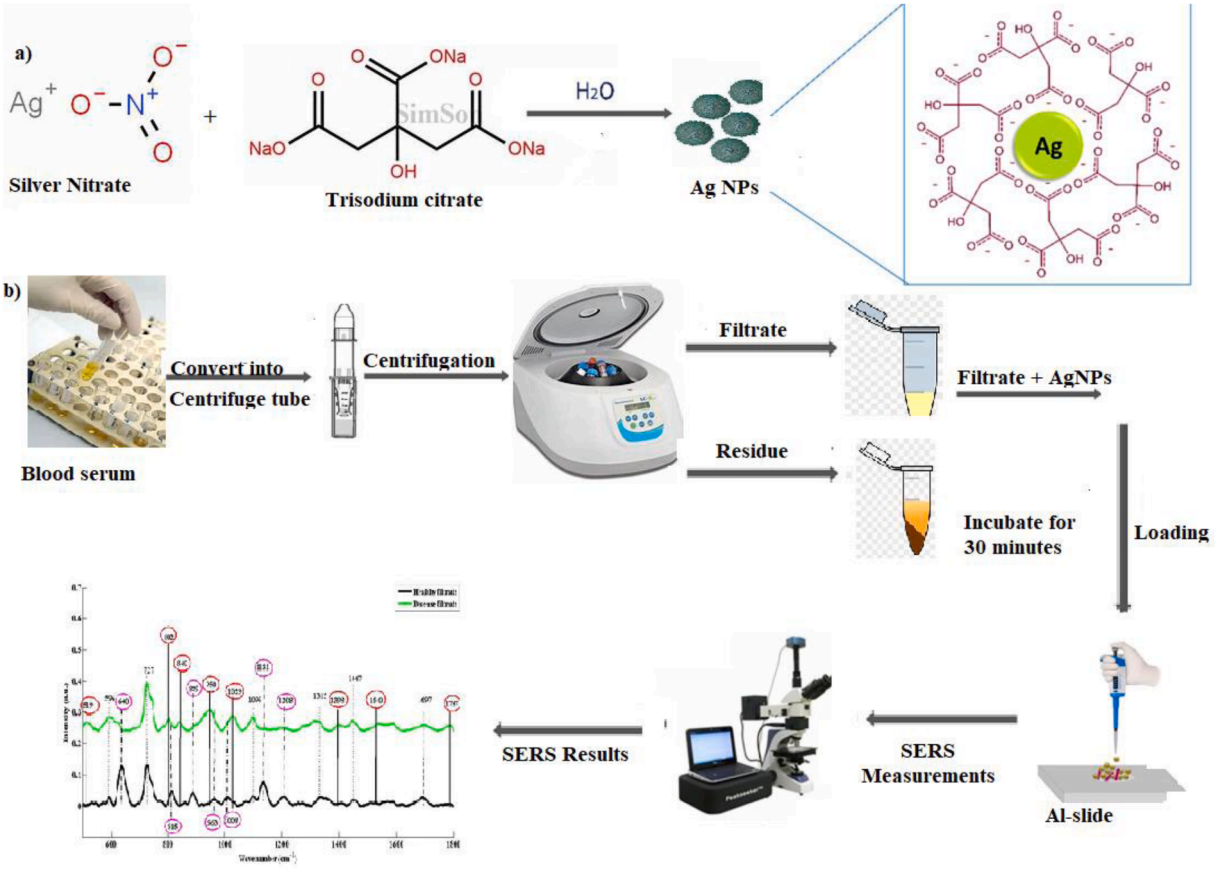

Fig. 1. Schematic illustration of the SERS analysis approach, demonstrating (a) Ag NPs synthesis and (b) serum fractionation by centrifugal filtration and SERS spectral acquisition using a 785 nm laser beam as a source of excitation.

typhimurium-related disease proteins range in size from 15 to 49 kDa. More than fifteen proteins having molecular weights in the range between 15 and 100 kDa are present in *Salmonella typhi* out of which eight major proteins are assigned molecular weights of 49, 43, 37, 35, 32, 30, 25, and 15 kDa [43] which can be a potential target after centrifugal filtration with the filter size of 50KDa, in the current study. So serum samples centrifugal filtration was performed to separate the LMWF and HMWF. The LMWF was then analyzed to determine the SERS spectral features associated with the disease biomarkers of typhoid.

Fever and other diseases alter the composition and concentration of certain biomolecules in human serum. The infections cause molecular changes in the blood that are accompanied by the emergence of some new molecules, such as antibodies, as well as an increase or decrease in the concentration of particular biomolecules in blood, which can ultimately be used for the diagnosis of disease through Raman spectroscopy [44]. SERS is used for the biomedical analysis of typhoid patients by which additional biomolecules are identified that are due to the *Salmonella typhi* bacterial biomolecules listed in Table 1.

Moreover, SERS based approach is established to compare the filtrate parts of blood serum samples of healthy individuals with typhoid patients to distinguish between them for the characterization of biochemical changes and diagnosis of typhoid disease. Furthermore, chemometric methods such as PCA are applied to detect qualitative differentiation and PLS-DA is used for the quantitative classification of the healthy versus typhoid-positive samples. This technique may be very helpful to detect the biochemical changes associated with the pathogens with high sensitivity and lead to the characterization and diagnosis of the disease.

2. Materials and methods

2.1. Ag-NPs preparation

The chemical reduction method was used to synthesize the Ag-NPs to be used as a substrate for SERS measurements. For this, 33.72 mg of $AgNO_3$ (silver nitrate) as a precursor was mixed with 200 mL de-ionized water to make a 1 mM solution, which was heated to a boil. 8 mL of 1% trisodium citrate ($Na_3C_6H_5O_7$), both as capping and reducing agent solution, was added, and the mixture was heated for a further 1 hour at constant stirring. The heating was then turned off and stirred the solution to bring it to room temperature. By adding deionized water, the total amount of 200 mL was maintained. The supernatant was separated through centrifuging 2 mL of nanoparticles suspension for 7 minutes at 600 rpm [45]. Electron microscopy was used to determine the shape and size of the grey-colored silver NPs and the methodology used for this is detailed in a paper [46].

2.2. Isolation of serum from the blood of typhoid patients and healthy individuals

The residual fluid component of blood after cells and blood clotting agents have been removed is called serum and it has proteins and other compounds [47]. To acquire serum, the blood was collected in a blood-storing tube and centrifugal separation was applied to separate components of blood. All of the samples were taken from PINUM hospital in Faisalabad, Pakistan. A total of 65 serum samples were collected, with 25 healthy and 40 typhoid blood serum samples.

2.3. Silver –NPs characterization

As reported in another study, transmission and scanning electron microscopy (TEM and SEM) were used to characterize the produced Ag-NPs by use of a field emission electron microscope (JEOL, JSM-7500F) [46]. To prepare the samples for TEM, a drop of an aqueous solution of silver NPs was slowly evaporated onto a carbon-layered copper grid (4 hundred mesh). Dry silver nanoparticles were put on a copper stump with no further conductive covering for SEM. The electron micrographs were analyzed using ImageJ software.

2.4. SERS spectral acquisition

SERS spectra were collected by an Optosky China Raman Microscope Spectrometer (ATR8300BS) with a 785 nm diode laser. For this, 25µl of each sample of filtrate portion of blood serum of healthy and *Salmonella typhi* positive was mixed with 25µl of Ag-nanoparticles followed by incubation for 30 minutes in an Eppendorf tube by the use of a

Table 1
SERS peak assignments were detected in the filtrate portions of blood serum samples of typhoid-positive and healthy individuals obtained by employing 50 KDa filters.

SERS Shift (cm^{-1})	Peak assignments	Component	Healthy Filtrate	Typhoid Filtrate	References
519	Phosphatidylinositol	Lipids	X	✓	[55]
596	Phosphatidylinositol	Lipids	✓	✓	[56]
640	Protein-tyrosine showing C-C twisting & C-S stretching	Proteins	✓	X	[57]
727	Collagen assignment that is due to proline, C-C stretching	Proteins	✓	✓	[58]
802	Ring breathing mode of DNA/RNA base which is thymine-based	DNA/RNA	X	✓	[59,60]
815	Tyrosine, Proline, hydroxyproline, ν_2 PO_2^- stretch in nucleic acids	Proteins, DNA/RNA	✓	X	[60]
840	α-Saccharide or band of α-Anomers Glucose saccharide	Carbohydrates	X	✓	[56]
889	Methylene rocking	Lipids	✓	X	[61]
950	Amino acids, & proline, valine single bond stretching vibrations	Proteins	X	✓	[62]
963	$CH'_{2,6}$ bending which is out of plane unassigned protein assignment	Proteins	✓	X	[63]
1008	pectin, phenylalanine	Proteins,	✓	X	[64]
1029	Due to methoxy group ($O\text{-}CH_3$) stretching	DNA/RNA	✓	✓	[65]
1096	Groups of PO_2^- (Phosphodioxy)	DNA/RNA	✓	✓	[56]
1131	Palmitic acid Fatty acid	Lipids	✓	X	[56]
1208	Proteins like phenylalanine or amide III, Tryptophan, $n(C\text{-}C_6H_5)$	Proteins	✓	X	[57,60,63,66]
1315	B, Z- a marker of DNA/RNA base Guanine	DNA/RNA	✓	✓	[67]
1398	CH_2 distortion or symmetric stretch of carbonyl C=O	Lipids	X	✓	[68]
1447	Different modes of vibrations such as deformation of CH_2 in lipids & protein CH_2 bending mode	Lipids, Proteins	✓	✓	[57,68]
1540	Due to the presence of aromatic hydrogen and vibrations of amide carbonyl (C=O) group	Proteins	✓	✓	[69]
1697	Turns & bands of Amide I	Proteins	✓	✓	[55]
1787	Lipid content	Lipids	X	✓	[70]

micropipette to allow the nanoparticles to interact adequately with the sample.

After incubation, a 30μl of the sample mixture was put on an aluminum (Al) slide using a micropipette for SERS data collection. The Raman excitation light was focused onto the sample using a 40 X objective lens and a laser power of 50 mW. The integration period per spectrum was set at 10 seconds to ensure that the results were stable, robust, and repeatable. At room temperature, 15 SERS spectra for each serum sample were acquired, with consistent conditions. Surface enhanced-RS spectra were obtained in the range of 400–1800cm^{-1}.

2.5. Pre-processing of SERS data

All of the fundamental pre-processing, including smoothing, removal of substrate, baseline correction, and vector normalization was performed using MATLAB R2009a (The MathWorks, USA) and its standard chemometric methods using in-house developed codes [48]. The data was smoothed using Savitzky-Golay filtering (S-G) using a 17th polynomial order and a 14-point window width [49]. The baseline of all SERS spectral data was adjusted using rubber band correction plus polynomial methods. The influence of the substrate of the aluminum slide was eliminated from SERS spectral data using the subtraction approach, followed by vector normalization.

2.6. Multivariate data analysis

Multivariate data analysis techniques including PCA and PLS-DA were used to examine SERS spectral data of filtrate portions of blood serum samples of healthy and typhoid patients. PCA is an un-supervised mathematical approach designed for qualitative multivariate data analysis, in which a lesser number of un-correlated variables (PCs or loadings) are obtained by transforming a greater number of original correlated variables, which do not take part much in decision making, into a smaller number of un-correlated variables (principal components or loadings). These principal components consist of all of the valuable information of Raman spectra [50]. The dimensionality of SERS data was decreased to obtain key Principal Components (PCs) to distinguish between healthy and disease-positive samples while maintaining their variability unchanged [51]. The 1st Principal Component (PC-1) always describes the most variation in the data, then the second Principal Component (PC-2), and so on [52]. PC loadings, which are used to differentiate SERS spectral data of typhoid from healthy samples, can be utilized to extract the orthogonal dimensions of data variability.

The PLS-DA is a supervised classifier algorithm that combines the partial least-square (PLS) and linear discriminant analysis (LDA) methodologies. The PLS-DA method is a statistical technique that can predict, categorize and explain as well as discriminate between SERS data sets having variability. It also has the benefit of being able to describe multidimensional datasets for a variety of reasons, including detecting various phases of the ailment in the medical area, assessing product quality assurance, and examining forensic medical examinations [53]. The definitive diagnosis of the classifier model as well as the utility of the method is mostly evaluated using the AUROC. The ROC curve is a graph that compares the false positive and true positive rates. The true positive rate is a measure of sensitivity, whereas the false positive rate is a measure of specificity [54].

3. Result and discussion

3.1. Mean SERS spectra of uncentrifuge versus centrifuge healthy samp1es

The mean spectrum of the whole serum sample (un-centrifuged healthy sample) in comparison with centrifuged (filtrate and residue) healthy sample and presented in the mean SERS spectra plot in Fig. 2. This helps to detect the distinct and characteristic SERS features that are particularly related to the biochemical changes taking place during the development of healthy serum samples, as well as the alterations that happened after centrifugation and removal of biomolecules/proteins bigger than 50KDa. These characteristic SERS features and their peak assignments are listed in Table 1 along with the references.

The characteristic SERS features present in un-centrifuged serum only are represented by dash-dot lines and categorized in a green box, including 573 cm^{-1}. The SERS spectral features that are present only in whole serum and filtrate are represented by dashed lines and categorized in red boxes, including 1096, 1315, and 1447 cm^{-1}. The SERS spectral features that increase in their intensities are represented by solid lines including, 596, 640, 815, 889, 1008, 1131, and 1208 cm^{-1}. SERS spectral features which go on decreasing in intensities designated by dotted lines are detected at 727, 963, and 1697 cm^{-1}.

All SERS bands of uncentrifuge and centrifuged blood serum samples are differentiated to detect the variations in the form of SERS characteristic peaks which are related to the changes taking place in the profile of blood serum after centrifugation. These differentiating SERS bands of known biological constituents/molecules are observed including stronger SERS signals at 640, 815, and 1208 cm^{-1}, and weaker signals at 963, 1008, and 1447 cm^{-1} can be assigned to healthy serum protein. The SERS characteristic peaks which differentiate whole serum from the filtrate fraction associated with healthy individuals are 573, 963, 1096, 1315, and 1447 cm^{-1}. Most of these peaks are related to nucleic acids

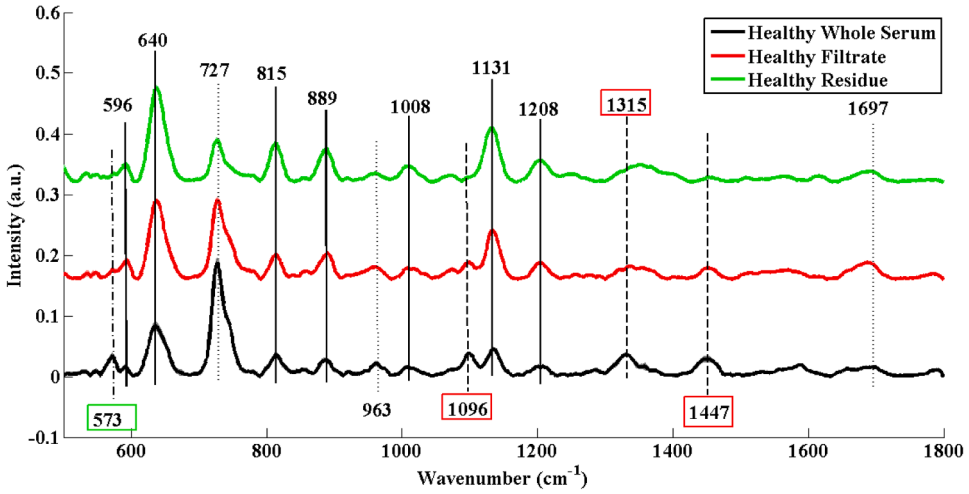

Fig. 2. Comparisons of mean SERS spectra of uncentrifuge, centrifuged (filtrate and residue) of healthy serum sample.

(DNA/RNA) and proteins. At 573 cm^{-1} the peaks appear due to the nucleic acid tryptophan, 596 cm^{-1} appear due to the Phosphatidylinositol, 727 cm^{-1} due to proline, 815 cm^{-1} due to tyrosine, 889 cm^{-1} due to methylene rocking, 963 cm^{-1} due to CH bending which is out of plane unassigned protein assignment, 1008 cm^{-1} due to polysaccharide, pectin, phenylalanine, 1096 cm^{-1} due to groups of PO_2^- (phosphodioxy), 1131 cm^{-1} due to fatty acid, 1208 cm^{-1} due to proteins like phenylalanine or amide III, tryptophan, n(C-C_6H_5), 1315 cm^{-1} due to guanine (B, Z-marker), 1447 cm^{-1} due to lipids cholesterol and it's esters shows different modes of vibrations like scissoring in CH_2 and bending in CH_3 and C-H and at 1697 cm^{-1} due to turns & bands of Amide-I.

In SERS spectra of uncentrifuge/whole blood serum sample, the peak intensities at 640, 889, and 1131 cm^{-1} are enhanced, while the peak intensities at 727 and 963 cm^{-1} are reduced and the bands at 573 cm^{-1} due to appear due to the nucleic acid tryptophan missing in centrifuged (filtrate and residue) while it is present in uncentrifuge/the whole spectrum. Notably, the peaks related to smaller molecules appearing in the filtrate and whole serum are due to the removal of proteins bigger than 50KDa which were not appearing in the residue due to the separation of these smaller proteins by 50KDa filters to be identified by SERS. These are peaks observed at 1096 cm^{-1} due to groups of PO_2^- (phosphodioxy), 1315 cm^{-1} due to guanine (B, Z-marker) and at 14477 cm^{-1} due to lipids cholesterol and its esters showing different modes of vibrations like scissoring in CH_2 and bending in CH_3 and C-H.

3.2. Mean SERS spectra of uncentrifuge versus centrifuge typhoid samp1es

All the SERS spectra of samples of filtrate portions of blood serum samples of typhoid positive and healthy persons have been preprocessed and mean SERS spectra are acquired for comparison.

The mean spectrum of the whole serum sample (un-centrifuged typhoid sample) in comparison with centrifuged (filtrate and residue) typhoid sample and presented in the mean SERS spectra plot in Fig. 3. This helps to detect the distinct and characteristic SERS features that are particularly related to the biochemical variations taking place during the development of typhoid disease, as well as the alterations that happened after centrifugation and removal of biomolecules/proteins bigger than 50KDa. These characteristic SERS features and their peak assignments are listed in Table 1 along with the references.

The characteristic SERS features present in un-centrifuged serum only are represented by dash-dot lines and categorized in red boxes, including 640, 898, and 1131 cm^{-1}. The SERS spectral features that increase in their intensities are represented by solid lines including, 678, 802, 840, 950, 1029, 1096, 1396and 1701cm^{-1}. SERS spectral features which go on decreasing in intensities designated by dotted lines are detected at 519, 596, 746, 1008, 1315, 1441, 1541and 1787 cm^{-1}. Furthermore, the peaks that are detected by a shift in the position shown by the dashed line include 727(vs) cm^{-1}.

All SERS bands of uncentrifuge and centrifuged blood serum samples are differentiated to detect the variations in the form of SERS characteristic peaks which are related to the variations taking place in the profile of blood serum after centrifugation. These differentiating SERS bands of known biological constituents/molecules are observed including stronger SERS signals at 746 and 802 cm^{-1} and weaker peaks signals at 678, and 1315 cm^{-1} can be assigned to bacterial DNA. The SERS characteristic peaks which differentiate whole serum from the filtrate fraction associated with the infection of *Salmonella typhi* are 640, 678, 727, 746, 898, 950, 1029, 1096, 1131, 1208, 1315, 1396, 1441, 1541, 1701 and 1787 cm^{-1}. Most of these peaks are related to nucleic acids (DNA/RNA) and proteins. At 519 and 596 cm^{-1} the peaks appear due to the Phosphatidylinositol, 727 cm^{-1} due to proline, stretching of C-C, 746 cm^{-1} due to thymine base ring breathing mode, 802 cm^{-1} due to ring breathing mode of DNA/RNA base which is thymine, 840 cm^{-1} due to α-saccharide; glucose saccharide, 950 cm^{-1} due to amino acids, polysaccharide and proline, valine single bond stretching vibrations, 1029 cm^{-1} due to methoxy group (O-CH_3) stretching, 1096 cm^{-1} due to groups of PO_2^- (phosphodioxy), 1208 cm^{-1} due to proteins like phenylalanine or amide III, tryptophan, n(C-C_6H_5), 1398 cm^{-1} due to CH_2 distortion or symmetric stretch of carbonyl C=O, 1441 cm^{-1} due to lipids cholesterol and it's esters shows different modes of vibrations like scissoring in CH_2 and bending in CH_3 and C-H, 1541 cm^{-1} due to aromatic hydrogens and amide carbonyl group vibrations, 1701 cm^{-1} due to glutamic acids and amino acids aspartic and 1787 cm^{-1} due to lipid contents.

In SERS spectra of uncentrifuge/whole blood serum sample, the peak intensities at 840, 950, and 1096 cm^{-1} are enhanced, while the peak intensities at 519, 596, and 1208 cm^{-1} are reduced and the bands at 678 cm^{-1} due to Guanine ring breathing mode is missing in uncentrifuge/whole one while it is present in both filtrate and residue. Notably, the peaks related to smaller molecules appearing in the filtrate are due to the removal of proteins bigger than 50KDa which were not appearing in the whole serum due to the dominance of these bigger proteins and were unable to be identified by SERS. There are additional peaks observed at 640 cm^{-1} (protein-tyrosine showing C-C twisting & C-S stretching), 898 cm^{-1} (C-O-C skeletal modes of monosaccharide & disaccharide), and at 1131 cm^{-1} (fatty acid) that are present only in un-centrifuged spectra while after centrifugation these features disappear.

3.3. Mean SERS spectra of Healthy vs diseased filtrates

Fig. 4 represents SERS mean plot of the filtrate portion of serum from

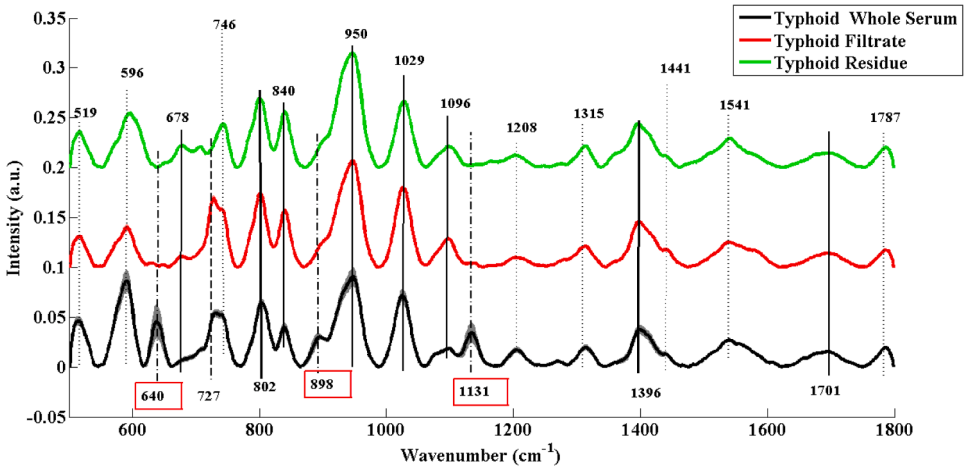

Fig. 3. Comparisons of mean SERS spectra of uncentrifuge, centrifuged (filtrate and residue) serum samples of patients positive for typhoid fever.

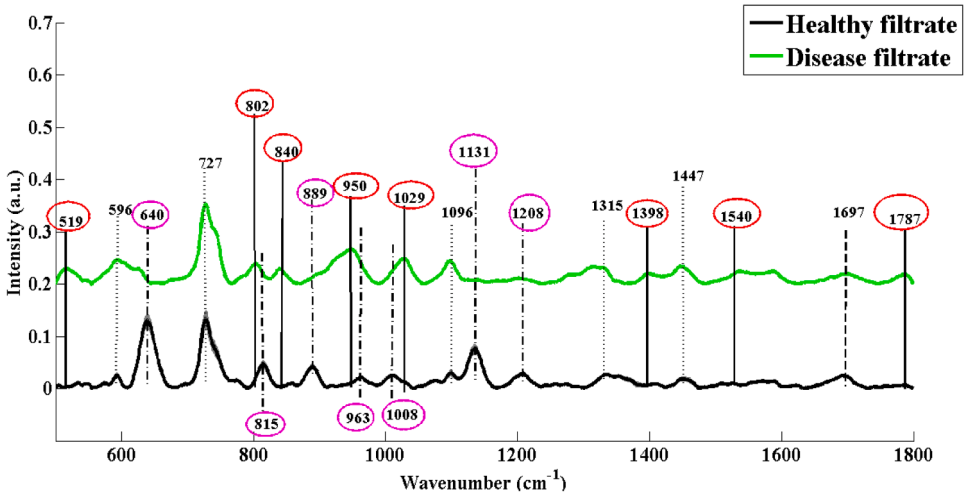

Fig. 4. Comparison of mean SERS spectra of healthy filtrate with the disease-positive filtrate.

healthy humans (black spectra) and typhoid samples (green spectra). The differentiating SERS characteristic features are designated as four types dash-dot, dashed, dotted, and solid lines. The peaks labeled with dash-dot lines are the characteristic peaks observed only in the healthy filtrate and categorized in purple circles. The solid lines are the characteristic peaks found only in typhoid-positive filtrate samples and categorized in red circles. The SERS features represented by dashed and solid lines are the characteristic peaks that are found in both healthy and disease-positive filtrate samples with decreasing and increasing peak intensities, respectively. These characteristic features are listed in Table 1 SERS bands of true healthy filtrate appear at 640, 815, 889, 963, 1008, 1131, 1208, and 1697 cm^{-1}. Most of these are related to proteins and lipids which give the basis for a quick distinction between healthy and disease-positive samples. At 640 cm^{-1} the peak intensity appears due to protein-tyrosine showing C-C twisting & C-S stretching, 815 cm^{-1} due to tyrosine, proline, hydroxyproline, ν_2 PO_2^- stretch in nucleic acids, 889 cm^{-1} due to methylene rocking, 963 cm^{-1} due to CH bending which is out of plane unassigned protein assignment, 1008 cm^{-1} due to polysaccharide, pectin, phenylalanine, 1131 cm^{-1} due to fatty acid and palmitic acid, 1208 cm^{-1} due to proteins like phenylalanine or amide III, tryptophan, n($C\text{-}C_6H_5$) and 1697 cm^{-1} due to turns & bands of Amide-I.

SERS bands of typhoid-positive filtrate samples appear at 519, 802, 840, 950, 1029, 1398, 1540, and 1787 cm^{-1}. Most of these peaks are related to proteins & lipids. The SERS band intensity at 519 cm^{-1} due to Phosphatidylinositol, at 802 cm^{-1} due to thymine ring breathing mode, 840 cm^{-1} due to α-saccharide or band of α-Anomers glucose saccharide, 950 cm^{-1} due to amino acids, polysaccharide & proline, valine, 1029 cm^{-1} due to methoxy group ($O\text{-}CH_3$) stretching,1398 cm^{-1} due to CH_2 distortion or symmetric stretch of carbonyl C=O,1540 cm^{-1} due to presence of aromatic hydrogen and vibrations of amide carbonyl (C=O) group and 1787 cm^{-1} due to lipid contents.

Those SERS features which are detected in both healthy and diseased filtrate are observed at 596, 727, 1096, 1315, and 1447 cm^{-1}. There are bands at 596 cm^{-1} due to Phosphatidylinositol, 727 cm^{-1} due to proline, 1096 cm^{-1} due to phosphodioxy groups, 1315 cm^{-1} due to B, Z- a marker of DNA/RNA base guanine and 1447 cm^{-1} due to different modes of vibrations such as deformation of CH_2 in lipids & protein CH_2 bending mode.

3.4. Principal component analysis (PCA)

For all healthy and typhoid-positive SERS spectral data sets, PCA was used as a differentiating method. PCA reduces the dimensionality of multi-dimensional datasets to reduce data complexities and transforms them into new variables called PCs that are orthogonal to each other. PCA, which may be used for objective identification between similar spectra, can highlight minor spectral changes. PCA was used in this study to see if SERS could be used to quickly differentiate between healthy and typhoid-infected patients by lowering the overall dimensionality of datasets.

The PCA scores and loadings for the dominating principal components (PCs) are plotted to explain variation in the SERS data sets. Fig. (a) illustrates a PCA scatter plot of SERS spectra of healthy and disease-positive samples. First Principal Component (PC-1) on the x-axis clusters and separates the SERS spectral data of the two groups of samples, which are shown with different colors. Black dots represent healthy SERS data, whereas green dots are shown for SERS data of typhoid-positive samples. Each dot represents one SERS spectrum and the PC-1 accounts for 71% of the total explained variation, whereas the second principal component accounts for 17% variability. The results show that PC-1 explains the most variation since it has distinctly grouped spectral datasets where healthy samples are on the negative side of PC-1, whereas on the positive side of PC-1 SERS spectra of typhoid samples are clustered indicating that both these samples are significantly different from the others based on its SERS features.

The analysis of PCA scores provides a visual representation of variability in the case of distinct clusters or groupings, but it does not give any information on the cause of the variation in data that differentiates data into different clusters. The PCA loadings are used to find the fundamental relationship in the original variables. The loadings can be designated as correlation coefficient vectors between variables in the original dataset, with each main component score. This illustrates specific characteristics that play a key role in the grouping/clustering of the SERS spectra of different samples. The large loadings either negative or positive of a variable make it significant for detection purposes since they play a significant influence in data variations concerning the associated PC when likened to the other variables. As can be seen in Fig. 5 (a), the disease-positive SERS spectra are grouped/clustered on the positive axis, whereas spectra of all other healthy samples are represented on the negative axis hence PC-1 positive and negative loadings are associated with typhoid disease and healthy samples respectively, allowing the PC-1 loadings to be used to identify whether a sample is healthy or infected.

PC-1 negative loadings related to spectral data of healthy samples, observed at 640 cm^{-1} (protein-tyrosine showing C-C twisting & C-S stretching), 815 cm^{-1} (tyrosine, proline, hydroxyproline, ν_2 PO_2^- stretch in nucleic acids), 889 cm^{-1} (methylene rocking), 963 cm^{-1} ($CH'_{2,6}$ bending protein assignment), 1008 cm^{-1} (phenylalanine), 1131 cm^{-1} (fatty acid and palmitic acid), 1208 cm^{-1} (phenylalanine, tryptophan) and 1697 cm^{-1} (Amide-I band). The PC-1 positive loadings could be

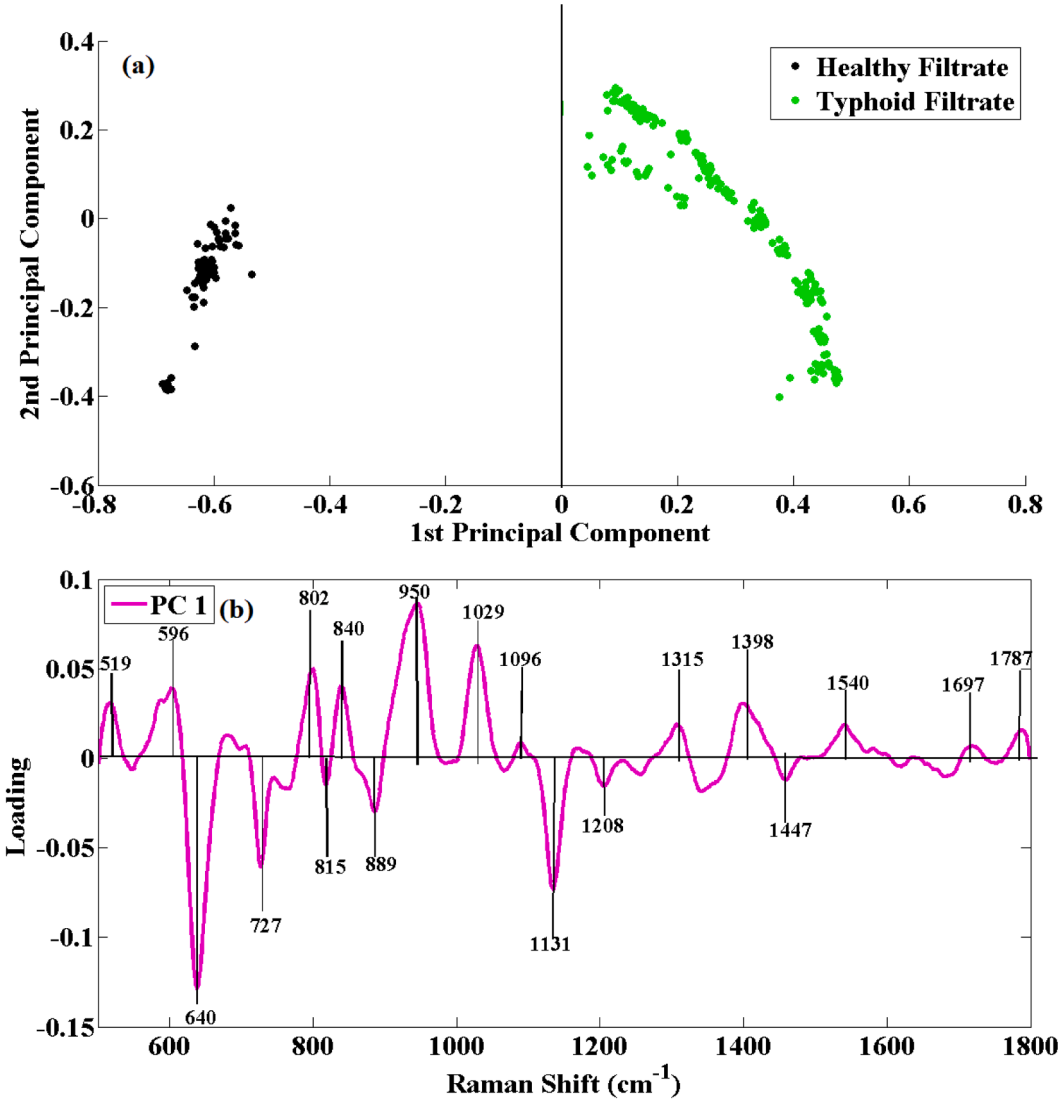

Fig. 5. (a) Principal component analysis scatter plot and (b) PCA loadings of SERS spectra of filtrate fractions of blood serum samples of healthy and typhoid fever patients.

related to spectral data of typhoid-infected samples observed at 519 cm^{-1} phosphatidylinositol, 802 cm^{-1} (thymine ring breathing mode), 840 cm^{-1} (band of α-Anomers glucose saccharide) and (α-saccharide), 950 cm^{-1} (amino acids, & proline, valine single bond stretching vibrations), 1029 cm^{-1} due to methoxy group (O-CH_3) stretching, 1398 cm^{-1} (CH_2 distortion or symmetric stretch of carbonyl C=O), 1540 cm^{-1} due to presence of aromatic hydrogen and vibrations of amide carbonyl (C=O) group and 1787 cm^{-1} (lipid contents). These conclusions are following mean spectra and demonstrate that SERS could be used to distinguish between filtrate portions of blood serum samples of healthy and typhoid-infected patients, based on respective spectral data variations.

3.5. Partial least square discriminant analysis (PLS-DA)

Analysis of PCA scores gives only visual distinction of SERS spectral data sets of all typhoid and healthy samples but it does not give any quantitative information about the data. PLS-DA is a data modeling approach that may be used for descriptive and predictive modeling as well as variable selection. PLS-DA is a supervised classification modeling approach that uses previous knowledge from classes to quantitatively discriminate between SERS spectra of healthy and typhoid-infected samples. To eliminate biased in the results, all data is put into a matrix and then randomized. PLS-DA is designed to take into account a large number of highly correlated elements and aids in unraveling underlying relationships between variables. PLS-DA works by the selection of the most discriminatory features in the spectral data sets that aid to categorize the samples into different classes like healthy and disease ones. PLS-DA accomplishes variable selection and classification in a single step using variables found in X data inside a supervised framework [71]. To construct the PLS-DA model, the SERS spectral data were divided into two sets, with 60% of the spectra of samples randomly selected and retained as the calibration set while 40% of the total data was used for testing. The variables with the least prediction error are identified and regarded as ideal latent variables (LVs) to attain a high level of accuracy in the results. The latent variables identified to be the optimum number for this purpose are 17. The class information was used as the y-variable and the spectral data as the x-variable to construct the PLS-DA classification model. To develop the model using the calibration dataset, the Bayes theorem and cross-validation were applied [52]. Cross-validation is used for validation, taking one sample (15 spectra) out of cross-validation and these spectra were not part of the calibration data. Because the validation dataset was maintained separate from the model training process, the trained classification model

was then used to verify its efficiency.

As shown in Fig. 6, the score plot differentiates between SERS spectral data sets of filtrate fractions of blood serum samples of healthy and *Salmonella typhi* infected samples. PLS-DA was designed to verify the accuracy of created classes. Healthy samples are clustered/grouped on the positive side of the line crossing the y-axis in SERS spectral datasets, while typhoid samples are grouped/clustered on the negative side. The black color indicates healthy, whereas the green color indicates SERS spectra of typhoid samples. PLS-DA has a measured validity of 97 %, precision of 76 %, sensitivity of 91 %, and specificity of 99 %, indicating that the model is valid and can be used to classify various typhoid samples and distinguish healthy samples from typhoid disease samples. Fig. 7 shows the ROC curve, which was used to evaluate the diagnostic capabilities of the SERS technique as well as the efficacy and functionality of the classifying model. The curve (ROC) was mapped among 1-specificity and sensitivity. The high efficiency of the model is demonstrated by its AUC value of 0.78. The highest AUC value is 1, indicating that the model is 100 percent valid, while a value of zero indicates that the model is invalid. Because the value of AUC of the SERS data set is close to 1, the PLS-DA graph describes the differences among the healthy and disease classes more clearly than the PCA scatter plot.

4. Discussion

The Raman spectra are greatly influenced by removing the bigger size proteins from the blood serum samples of the healthy and typhoid-positive patients by using 50KDa filters and the filtrate parts of these samples are characterized by the SERS technique. The cellulose membrane separated the dominant large molecular weight proteins(LMW) from the smaller molecules, allowing for more efficient SERS spectroscopic detection [72].

The intensity of bands associated with lipids is located at 519, 596, 1131, and 1447 cm^{-1}. At 519 cm^{-1} the peak intensity is only present in typhoid filtrate and not found in healthy filtrate due to bacterial cholesterol (phosphatidylinositol). Phosphatidylinositol-4-phosphate [PI(4)P] is a signaling molecule present on the plasma membranes, Golgi, and endosomes of bacteria that plays a significant part in trafficking, phagolysosome resolution, inflammasome development, and autophagy [73]. The peak intensity at 596 cm^{-1} is present both in healthy and diseased samples but the intensity of the band increase due to the phosphatidylinositol of bacteria as well as the human itself as in humans, 4 membrane-related to phos-phatidylinositol-4-kinases (PI4Ks) plus a single preserved PI(4)P phosphatase, work together to maintain homeostasis [74]. The band intensity at 1131 cm^{-1} is also lipids (palmitic acid and fatty acid) which are not found in *Salmonella typhi* positive samples. At 1787 cm^{-1} the peak is also due to bacterial lipid contents.

The carbohydrates (polysaccharides, pectin) differentiating feature observed at 1008 cm^{-1} is detected in healthy samples only [75] while bacterial carbohydrates peaks observed at 840 cm^{-1} due to α-saccharide or band of α-Anomers glucose saccharide. These carbohydrates act as adhesion receptors in the early stages of bacterial infections. The role of carbohydrates in *Salmonella enterica* infection and the production of fimbrial adhesions by different bacterial species. Carbohydrates are used by these microbes as receptors for infection; although, the carbohydrate consumption of microbes differs. Various carbohydrate moieties are found on the surface of the mucosal tissues of the gastrointestinal system and play a significant role in infection, serving as the site of contamination or route of entrance for most microorganisms. Carbohydrates are used by bacteria throughout their infection and/or invasion processes. They can serve as receptors for a variety of bacteria as well as a barrier against infection [76].

The SERS bands associated with DNA/RNA are observed in both healthy and typhoid-positive filtrate fractions including 1096 cm^{-1} due to phosphodioxy groups and 1315 cm^{-1} (Guanine) have intensities increased in typhoid-positive filtrate fractions as compared to healthy ones indicating that this increase in DNA/RNA contents may be due to presence of bacteria as infection in the filtrate fractions of blood serum samples. The DNA/RNA band at 815 cm^{-1} is due to ν_2 PO_2^- stretch in nucleic acids only found in healthy filtrate fractions. Moreover, the SERS features which are found only in typhoid-positive filtrate fractions are observed at 802 cm^{-1} due to thymine ring breathing mode, and 1029 cm^{-1} due to methoxy group (O-CH_3) stretching. The bacteria, *Salmonella typhi*, during infection, induces death and sepsis in various cells by making active toll receptors, which are the source of cell-free DNA in the blood serum. The characteristic SERS features of cell-free DNA are considered indications of specific disorders [77].

Some SERS spectral features are related to proteins. The SERS features having an increase in intensities in typhoid-positive filtrate fractions as compared to healthy ones associated with proteins are found at

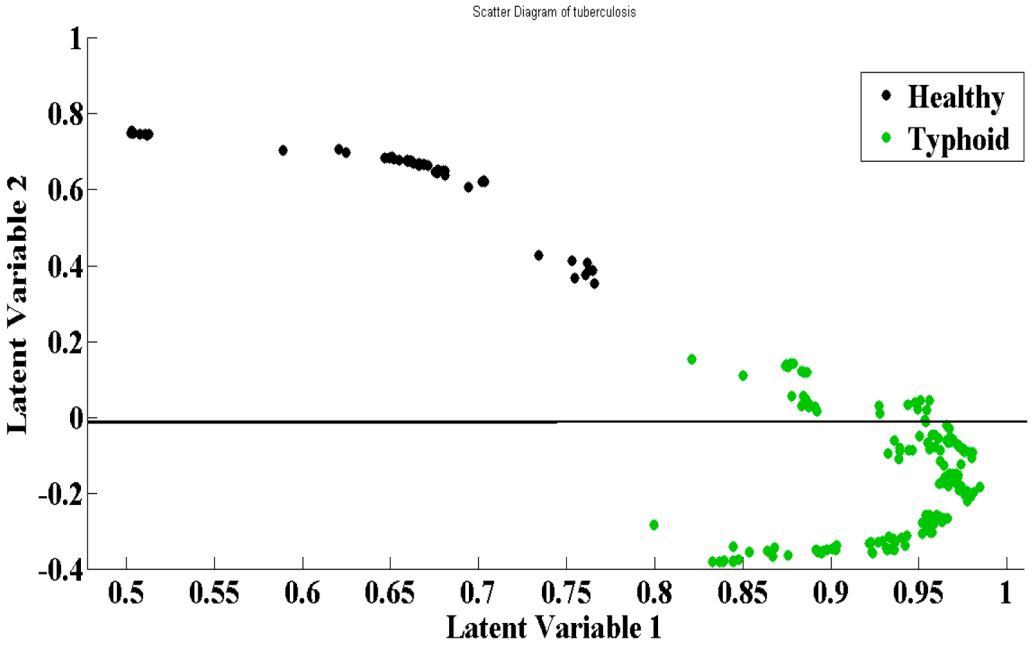

Fig. 6. Score plot of the PLS-DA model for validation SERS spectral dataset of filtrate fractions healthy and typhoid fever.

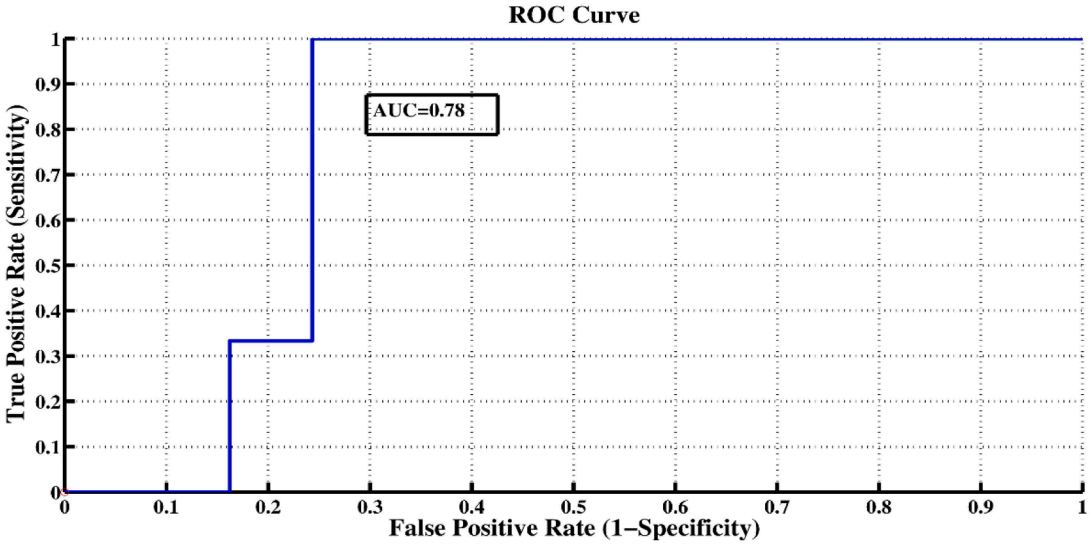

Fig. 7. Receiver operating characteristics (ROC) curve for the efficiency of the PLS-DA model developed for the SERS spectra of filtrate fractions of healthy and typhoid fever.

727 cm^{-1} due to proline and 1447 cm^{-1} due to different modes of vibrations such as protein CH_2 bending mode. The decreasing band intensity is present at 1697 cm^{-1} (protein contents). The SERS bands associated with proteins which are only observed n healthy samples are present at 640 cm^{-1} due to protein-tyrosine, 815 cm^{-1} due to proline, hydroxyproline, 963 cm^{-1} due to CH bending which is out of plane unassigned protein assignment, 1008 cm^{-1} due to pectin, phenylalanine and 1208 cm^{-1} due to proteins like phenylalanine or amide III and those which are solely present disease samples are at 950 cm^{-1} due to amino acids, proline, valine single bond stretching vibrations and 1540 cm^{-1} due to the presence of aromatic hydrogen and vibrations of amide carbonyl (C=O) group respectively. These differentiating SERS features between healthy and typhoid patients also indicate the potential of the SERS technique for the characterization of the filtrate fractions of the respective blood serum samples.

5. Conclusions

Surface-enhanced Raman spectroscopy using Ag-nanoparticles SERS substrate is found to be an excellent technique for the quick identification and evaluation of filtrate portions of the blood serum samples of healthy and typhoid samples for disease diagnosis. The characteristic SERS bands have been observed in disease-positive samples that may be linked to the development of infection by *Salmonella typhi* bacteria. These bands are associated with carbohydrates, lipids, nucleic acid, and proteins. PCA was found to be highly useful for qualitatively distinguishing healthy and pathological SERS spectral data sets. The diagnostic capability of SERS to quantitatively differentiate between filtrate fractions of healthy and typhoid patients has been found excellent. To categorize various healthy and typhoid filtrate fractions, the PLS-DA model is successfully established with 97 % accuracy, 76 % precision, 91 % sensitivity, and 99 % specificity. The centrifugal filtration approach is found very useful for analyzing the smaller, potentially disease-related proteins, more effectively and to avoid the interference of the bigger size proteins which may dominate if not removed.

CRediT authorship contribution statement

Maria Akram: Writing – original draft. **Muhammad Irfan Majeed:** Supervision. **Haq Nawaz:** Conceptualization. **Nosheen Rashid:** Investigation. **Muhammad Rizwan Javed:** Validation. **Muhammad Zeeshan Ali:** Data curation. **Ali Raza:** Software. **Muhammad Shakeel:** Software. **Hafiz Mahmood ul Hasan:** Software. **Zain Ali:** Formal analysis. **Usama Ehsan:** Formal analysis. **Muhammad Shahid:** Formal analysis.

Declaration of Competing Interests

The authors have no known competing financial interests or personal relationships that could have appeared to influence the work reported in this paper.

Funding information

This research did not receive any specific grant from funding agencies in the public, commercial, or not-for-profit sectors.

References

[1] S. Hosoglu, et al., Risk factors for enteric perforation in patients with typhoid fever, Am. J. Epidemiol. 160 (1) (2004) 46–50.
[2] C. Ansong, et al., Proteomics analysis of the causative agent of typhoid fever, J. Proteome Res. 7 (2) (2008) 546–557.
[3] G.W. Brunette, CDC health information for international travel 2012: The Yellow Book, Oxford University Press, 2011.
[4] G.C. Buckle, C.L.F. Walker, R.E. Black, Typhoid fever and paratyphoid fever: systematic review to estimate global morbidity and mortality for 2010, J. Glob. Health 2 (1) (2012).
[5] A.K. Bhunia, Salmonella enterica. Foodborne Microbial Pathogens, Springer, 2018, pp. 271–287.
[6] R.K. Esena, E. Owusu, Quality of cooked foods in urban schools in Ghana: Review of food borne diseases and health implications, Int. J. Sci. Technol. Res. 2 (2013) 267–275.
[7] S. Gopinath, S. Carden, D. Monack, Shedding light on Salmonella carriers, Trends Microbiol. 20 (7) (2012) 320–327.
[8] L.A. Knodler, J.R. Elfenbein, Trends Microbiol. 27 (11) (2019) 964–965.
[9] G. Andualem, et al., A comparative study of Widal test with blood culture in the diagnosis of typhoid fever in febrile patients, BMC Res. Notes 7 (1) (2014) 1–6.
[10] Z. Begum, et al., Evaluation of Typhidot (IgM) for early diagnosis of typhoid fever, J. Med. Microbiol. 3 (1) (2009) 10–13.
[11] J. Felgner, et al., Development of ELISAs for diagnosis of acute typhoid fever in Nigerian children, PLoS Negl.Trop. Dis. 11 (6) (2017), e0005679.
[12] F. Fan, et al., The development and evaluation of a loop-mediated isothermal amplification method for the rapid detection of *Salmonella enterica serovar Typhi*, PLoS One 10 (4) (2015), e0124507.
[13] I.U. Khan, et al., Comparative diagnosis of typhoid fever by polymerase chain reaction and widal test in Southern Districts (Bannu, Lakki Marwat and DI Khan) of Khyber Pakhtunkhwa, Pakistan, Acta Sci. Malaysia 1 (2) (2017) 12–15.
[14] N. Cheng, et al., Nanozyme-mediated dual immunoassay integrated with smartphone for use in simultaneous detection of pathogens, ACS Appl. Mater. Interfaces 9 (46) (2017) 40671–40680.

[15] J.R. Andrews, E.T. Ryan, Diagnostics for invasive Salmonella infections: current challenges and future directions, Vaccine 33 (2015) C8–C15.
[16] S. Stöckel, et al., The application of Raman spectroscopy for the detection and identification of microorganisms, J. Raman Spectrosc. 47 (1) (2016) 89–109.
[17] C. Fan, et al., Rapid detection of food-and waterborne bacteria using surface-enhanced Raman spectroscopy coupled with silver nanosubstrates, Appl. Microbiol. Biotechnol. 92 (5) (2011) 1053–1061.
[18] M. Kahraman, et al., Convective assembly of bacteria for surface-enhanced Raman scattering, Langmuir 24 (3) (2008) 894–901.
[19] L. Zeiri, et al., Surface-enhanced Raman spectroscopy as a tool for probing specific biochemical components in bacteria, Appl. Spectrosc. 58 (1) (2004) 33–40.
[20] Y. Cheong, et al., Rapid label-free identification of Klebsiella pneumoniae antibiotic resistant strains by the drop-coating deposition surface-enhanced Raman scattering method, Spectrochim. Acta Part A 183 (2017) 53–59.
[21] J. Li, et al., Label-free identification carbapenem-resistant Escherichia coli based on surface-enhanced resonance Raman scattering, RSC Adv. 8 (9) (2018) 4761–4765.
[22] F.U. Ciloglu, et al., Identification of methicillin-resistant Staphylococcus aureus bacteria using surface-enhanced Raman spectroscopy and machine learning techniques, Analyst 145 (23) (2020) 7559–7570.
[23] S. Preciado-Flores, et al., SERS spectroscopy and SERS imaging of Shewanella oneidensis using silver nanoparticles and nanowires, Chem. Commun. 47 (14) (2011) 4129–4131.
[24] X. Chen, et al., Surface-enhanced Raman scattering method for the identification of methicillin-resistant Staphylococcus aureus using positively charged silver nanoparticles, Microchim. Acta 186 (2) (2019) 102.
[25] Y. Yan, et al., Improvement of surface-enhanced raman scattering method for single bacterial cell analysis, Front. Bioeng. Biotechnol. 8 (2020) 1091.
[26] G. Naja, et al., Raman-based detection of bacteria using silver nanoparticles conjugated with antibodies, Analyst 132 (7) (2007) 679–686.
[27] D.D. Galvan, Q. Yu, Surface-Enhanced Raman Scattering for Rapid Detection and Characterization of Antibiotic-Resistant Bacteria, Adv. Healthc. Mater. 7 (13) (2018), 1701335.
[28] D. Yang, et al., Reproducible E. coli detection based on label-free SERS and mapping, Talanta 146 (2016) 457–463.
[29] H. Nargis, et al., Comparison of surface enhanced Raman spectroscopy and Raman spectroscopy for the detection of breast cancer based on serum samples, Spectrochim. Acta Part A 246 (2021), 119034.
[30] M. Tahira, et al., Surface-enhanced Raman spectroscopy analysis of serum samples of typhoid patients of different stages, Photodiagn. Photodyn. Ther. 34 (2021), 102329.
[31] S. Ahmad, et al., Characterization and prediction of viral loads of Hepatitis B serum samples by using surface-enhanced Raman spectroscopy (SERS), Photodiagn. Photodyn. Ther. 35 (2021), 102386.
[32] S. Tabbasum, et al., Surface-enhanced Raman spectroscopy for comparison of serum samples of typhoid and tuberculosis patients of different stages, Photodiagn. Photodyn. Ther. 35 (2021), 102426.
[33] S. Akbar, et al., Surface-Enhanced Raman Spectroscopic (SERS) Characterization of Low Molecular Weight Fraction of the Serum of Breast Cancer Patients with Principal Component Analysis (PCA) and Partial Least Square-Discriminant Analysis (PLS-DA), Anal. Lett. 55 (10) (2022) 1588–1604.
[34] R.Z.A. Bari, et al., Surface-enhanced Raman spectroscopic analysis of centrifugally filtered HBV serum samples, Photodiagn. Photodyn. Ther. 38 (2022), 102808.
[35] J.-S. Lee, et al., Silver nanoparticle− oligonucleotide conjugates based on DNA with triple cyclic disulfide moieties, Nano Lett. 7 (7) (2007) 2112–2115.
[36] Y. Shen, et al., Characterization of the human blood plasma proteome, Proteomics 5 (15) (2005) 4034–4045.
[37] M. Leeman, et al., Proteins and antibodies in serum, plasma, and whole blood—size characterization using asymmetrical flow field-flow fractionation (AF4), Anal. Bioanal.Chem. 410 (20) (2018) 4867–4873.
[38] D.R. Parachalil, et al., Raman spectroscopic screening of high and low molecular weight fractions of human serum, Analyst 144 (14) (2019) 4295–4311.
[39] N.L. Anderson, et al., The human plasma proteome: a nonredundant list developed by combination of four separate sources, Mol. Cell. Proteomics 3 (4) (2004) 311–326.
[40] F. Bonnier, M.J. Baker, H.J. Byrne, Vibrational spectroscopic analysis of body fluids: avoiding molecular contamination using centrifugal filtration, Anal. Methods 6 (14) (2014) 5155–5160.
[41] J.M. Cameron, et al., Vibrational spectroscopic analysis and quantification of proteins in human blood plasma and serum, Vib. Spectrosc. Protein Res. (2020) 269–314.
[42] A. Alpert, A. Shukla, Precipitation of large, high-abundance proteins from serum with organic solvents, Assoc. Biomol. Resource Facilities (ABRF) (2003). P111-W.
[43] N. Hamid, S. Jain, Characterization of an outer membrane protein of Salmonella enterica serovar Typhimurium that confers protection against typhoid, Clin. Vaccine Immunol. 15 (9) (2008) 1461–1471.
[44] S. Kumar, et al., Raman and infra-red microspectroscopy: towards quantitative evaluation for clinical research by ratiometric analysis, Chem. Soc. Rev. 45 (7) (2016) 1879–1900.
[45] H. Fang, et al., Ultrasensitive and quantitative detection of paraquat on fruits skins via surface-enhanced Raman spectroscopy, Sens. Actuators B 213 (2015) 452–456.
[46] M. Kashif, et al., Surface Enhanced Raman Spectroscopy of the serum samples for the diagnosis of Hepatitis C and prediction of the viral loads, Spectrochim. Acta Part A 242 (2020), 118729.
[47] M.K. Tuck, et al., Standard operating procedures for serum and plasma collection: early detection research network consensus statement standard operating procedure integration working group, J. Proteome Res. 8 (1) (2009) 113–117.
[48] H. Nawaz, et al., Evaluation of the potential of Raman microspectroscopy for prediction of chemotherapeutic response to cisplatin in lung adenocarcinoma, Analyst 135 (12) (2010) 3070–3076.
[49] H. Nawaz, et al., Prediction of viral loads for diagnosis of Hepatitis C infection in human plasma samples using Raman spectroscopy coupled with partial least squares regression analysis, J. Raman Spectrosc. 48 (5) (2017) 697–704.
[50] E. Witkowska, et al., Strain-level typing and identification of bacteria–a novel approach for SERS active plasmonic nanostructures, Anal. Bioanal.Chem. 410 (20) (2018) 5019–5031.
[51] X. Wu, et al., Differentiation and classification of bacteria using vancomycin functionalized silver nanorods array based surface-enhanced Raman spectroscopy and chemometric analysis, Talanta 139 (2015) 96–103.
[52] X. Wu, et al., Detection and differentiation of foodborne pathogenic bacteria in mung bean sprouts using field deployable label-free SERS devices, Analyst 138 (10) (2013) 3005–3012.
[53] F. Westad, F. Marini, Validation of chemometric models–a tutorial, Anal. Chim. Acta 893 (2015) 14–24.
[54] T. Zelmanovitz, et al., The receiver operating characteristics curve in the evaluation of a random urine specimen as a screening test for diabetic nephropathy, Diabetes Care. 20 (4) (1997) 516–519.
[55] R.J. Lakshmi, et al., Tissue Raman spectroscopy for the study of radiation damage: brain irradiation of mice, Radiat. Res. 157 (2) (2002) 175–182.
[56] C. Krafft, et al., Near infrared Raman spectra of human brain lipids, Spectrochim. Acta Part A 61 (7) (2005) 1529–1535.
[57] J.W. Chan, et al., Micro-Raman spectroscopy detects individual neoplastic and normal hematopoietic cells, Biophys. J. 90 (2) (2006) 648–656.
[58] C.J. Frank, R.L. McCreery, D.C. Redd, Raman spectroscopy of normal and diseased human breast tissues, Anal. Chem. 67 (5) (1995) 777–783.
[59] S. Farquharson, et al., Analysis of 5-fluorouracil in saliva using surface-enhanced Raman spectroscopy, J. Raman Spectrosc. 36 (3) (2005) 208–212.
[60] W.T. Cheng, et al., Micro-Raman spectroscopy used to identify and grade human skin pilomatrixoma, Microsc. Res. Tech. 68 (2) (2005) 75–79.
[61] Z. Huang, et al., Raman spectroscopy in combination with background near-infrared autofluorescence enhances the in vivo assessment of malignant tissues, Photochem. Photobiol. 81 (5) (2005) 1219–1226.
[62] M. Gniadecka, et al., Diagnosis of basal cell carcinoma by Raman spectroscopy, J. Raman Spectrosc. 28 (2-3) (1997) 125–129.
[63] Z. Huang, et al., Near-infrared Raman spectroscopy for optical diagnosis of lung cancer, Int. J. Cancer 107 (6) (2003) 1047–1052.
[64] Naumann, D. *Infrared and NIR Raman spectroscopy in medical microbiology*. in *Infrared spectroscopy: new tool in medicine*. 1998. International Society for Optics and Photonics.
[65] H. Schulz, M. Baranska, Identification and quantification of valuable plant substances by IR and Raman spectroscopy, Vib. Spectrosc. 43 (1) (2007) 13–25.
[66] E. Katainen, et al., Quantification of the amphetamine content in seized street samples by Raman spectroscopy, J. Forensic Sci. 52 (1) (2007) 88–92.
[67] A. Ruiz-Chica, et al., Characterization by Raman spectroscopy of conformational changes on guanine–cytosine and adenine–thymine oligonucleotides induced by aminooxy analogues of spermidine, J. Raman Spectrosc. 35 (2) (2004) 93–100.
[68] E.O. Faolain, et al., A study examining the effects of tissue processing on human tissue sections using vibrational spectroscopy, Vib. Spectrosc. 38 (1-2) (2005) 121–127.
[69] B.R. Wood, et al., FTIR microspectroscopic study of cell types and potential confounding variables in screening for cervical malignancies, Biospectroscopy 4 (2) (1998) 75–91.
[70] D. Kaushik, B. Michniak-Kohn, Percutaneous penetration modifiers and formulation effects: thermal and spectral analyses, AAPS PharmSciTech 11 (3) (2010) 1068–1083.
[71] J. Barrera, et al., Improved detection of anti-HCV in post-transfusion hepatitis by a third-generation ELISA, Vox Sang. 68 (1) (1995) 15–18.
[72] R.L. Sparrow, D.W. Greening, R.J. Simpson, A protocol for the preparation of cryoprecipitate and cryodepleted plasma. Serum/Plasma Proteomics, Springer, 2011, pp. 259–265.
[73] G. Miao, et al., The ER-localized transmembrane protein TMEM39A/SUSR2 regulates autophagy by controlling the trafficking of the PtdIns (4) P phosphatase SAC1, Mol. Cell 77 (3) (2020) 618–632, e5.
[74] L.M. Del Bel, J.A. Brill, Sac1, a lipid phosphatase at the interface of vesicular and nonvesicular transport, Traffic 19 (5) (2018) 301–318.
[75] G. Shetty, et al., Raman spectroscopy: elucidation of biochemical changes in carcinogenesis of oesophagus, Br. J. Cancer 94 (10) (2006) 1460–1464.
[76] Kato, K. and A. Ishiwa, *Roles of carbohydrates in the infection strategies of enteric pathogens*. Tropical medicine and health, 2014.
[77] D.R.D. Andrade, D.R.D. Andrade Júnior, Typhoid fever as cellular microbiological model, 45, Revista do Instituto de Medicina Tropical de São Paulo, 2003, pp. 185–191.